The simplest ENSO recharge oscillator

Gerrit Burgers
Royal Netherlands Meteorological Institute (KNMI), De Bilt, Netherlands

Fei-Fei Jin
Florida State University, Tallahassee, Florida, USA

Geert Jan van Oldenborgh
Royal Netherlands Meteorological Institute (KNMI), De Bilt, Netherlands

Received 10 March 2005; revised 1 June 2005; accepted 9 June 2005; published 13 July 2005.

[1] Eastern Pacific sea surface temperature (SST) and mean equatorial Pacific thermocline depth are key variables in El Niño–Southern Oscillation (ENSO). A linear fit to observations leads to a remarkably simple picture: ENSO can be represented by a classical damped oscillator, with SST and thermocline depth playing the roles of momentum and position, respectively. An independent fit of observed relationships between western and eastern thermocline depth, central wind stress and eastern Pacific SST yields the same picture and supports a recharge oscillator interpretation. The oscillation arises from the interaction between the recharge time of the Warm Pool and the time delay between east and west Pacific. Both finite Kelvin wave speed and SST dynamics contribute to the time delay. Including seasonality in the description, we find two periods of relative instability: boreal spring, with a large phase progression, and autumn, with nearly stationary phase.
Citation: Burgers, G., F.-F. Jin, and G. J. van Oldenborgh (2005), The simplest ENSO recharge oscillator, *Geophys. Res. Lett.*, *32*, L13706, doi:10.1029/2005GL022951.

1. Introduction

[2] Our understanding of the mechanism of ENSO has deepened over the years, see, for example, the review by *Neelin et al.* [1998]. Two well-known pictures for the basic El Niño mechanisms are the delayed oscillator of *Suarez and Schopf* [1988] and *Battisti and Hirst* [1989] and the recharge oscillator of *Jin* [1996, 1997]. In the recharge oscillator, the fast propagation processes are explicitly filtered to emphasize the collective effect of tropical ocean waves. Natural variables are eastern Pacific sea surface temperature T_E and the mean thermocline depth h. *Meinen and McPhaden* [2000] found that observations roughly follow circular paths in $T_E - h$ space, confirming the phase relationship of the recharge oscillator picture. While *Kessler* [2002] questioned whether it is appropriate to speak of oscillations in the observations, *Philander and Fedorov* [2003] and *Fedorov et al.* [2003] argue that ENSO corresponds to a stable oscillatory system excited by noise. The two main variables of the system, the work done on the ocean by the winds and the perturbation available potential energy of the ocean, are closely related to T_E and h.

0094-8276/05/2005GL022951$05.00

[3] In the original formulation of *Jin* [1997], the tilt of the thermocline reacts instantaneously to the wind stress, and wind stress reacts instantaneously to SST. *Mechoso et al.* [2003] propose a version that includes a spin-up time for the reaction of wind stress to SST. In this paper, we include a parameterization of the fast wave process by which the thermocline tilt adjusts to the wind stress into the recharge oscillator. We show that the original recharge oscillator is a special case of an extended recharge oscillator model, which is formulated in terms of four equations for four basic variables. The four equations can be reduced to two equations in terms of eastern Pacific SST and mean equatorial thermocline depth. Next, following an approach that is similar to *Mechoso et al.* [2003], we show that the parameters of the four-equation system not only can be fitted to describe the observations fairly well but also are consistent with parameters obtained from a fit to the two-equations system. Moreover, the recharge oscillator has a particular simple form when formulated in scaled variables, with clear Bjerknes and Wyrtki feedbacks setting the decay timescale and period of ENSO, and a negligible damping on mean equatorial thermocline anomalies. Finally, we discuss the considerable seasonal dependence of the parameters of the two-equation system.

2. Extended Recharge Oscillator

[4] The recharge oscillator of *Jin* [1997] is based on four equations for the western Pacific thermocline depth anomaly h_W, the eastern Pacific thermocline depth anomaly h_E, the central Pacific zonal wind stress anomaly τ, and the eastern Pacific SST anomaly T_E. There are two prognostic equations and two diagnostic equations:

$$\begin{aligned} \frac{d}{dt} h_W &= -r(h_W + \alpha\tau) \\ \frac{d}{dt} T_E &= -\epsilon_1 (T_E - \gamma_h h_E) \\ \tau &= b T_E \\ h_E &= h_W + \tau. \end{aligned} \tag{1}$$

Units are chosen such that the coefficient of τ in the last equation equals one. The first equation gives the collective response of the western Pacific to wind stress changes through Kelvin waves, Rossby waves and western boundary reflection, the last equation states that the tilt of the

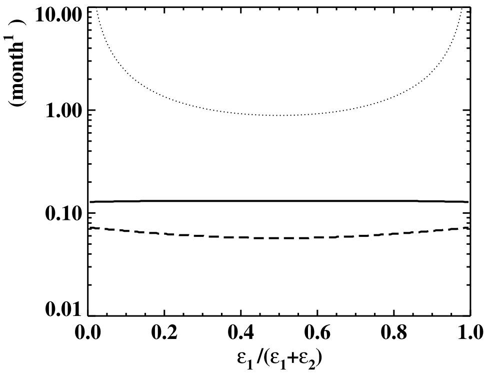

Figure 1. Eigenvalues of the system of equations (3) as a function of $\epsilon_1/(\epsilon_1 + \epsilon_2)$ for fixed $\epsilon_1^{-1} + \epsilon_2^{-1}$. The solid and dashed lines denote the imaginary part and the decay rate of the pair of complex eigenvalues; the dotted line denotes the fast decay rate.

thermocline reacts quasi-instantaneously to wind stress. In this version of the recharge oscillator, the first prognostic equation is that of western Pacific thermocline depth, the second the equation that describes the reaction of eastern Pacific SST to eastern Pacific thermocline depth.

[5] The mismatch between wind stress and thermocline slope is an important factor for interannual variability [*Neelin et al.*, 1998]. In (1), the mismatch is caused by the prognostic T_E equation. An alternative is that the mismatch is caused by the finite time it takes for a Kelvin wave to propagate a signal from the central Pacific to the east, while T_E reacts instantaneously to h_E. This can be described by:

$$\begin{aligned} \frac{d}{dt}h_W &= -r(h_W + \alpha\tau) \\ T_E &= \gamma_h h_E \\ \tau &= bT_E \\ \frac{d}{dt}h_E &= -\epsilon_2(h_E - h_W - \tau). \end{aligned} \tag{2}$$

[6] Eliminating τ and h_E, both (1) and (2) reduce to the same mathematical form, although physically the origin of the second timescale is quite different. In reality, both the time it takes for a Kelvin wave to cross the Pacific and the time it takes for SST to react to thermocline depth play a role [*Zelle et al.*, 2004]. A natural generalization that covers both the original recharge oscillator and the version with the relaxation time for h_E is:

$$\begin{aligned} \frac{d}{dt}h_W &= -r(h_W + \alpha\tau) \\ \frac{d}{dt}T_E &= -\epsilon_1(T_E - \gamma_h h_E) \\ \tau &= bT_E \\ \frac{d}{dt}h_E &= -\epsilon_2(h_E - h_W - \tau). \end{aligned} \tag{3}$$

This generalization is similar to that proposed by *Mechoso et al.* [2003], who added an adjustment timescale to the atmosphere rather than to the h_E equation.

[7] The set of equations (3) has for a wide range of parameters one pair of slowly decaying eigenmodes, and one fast mode with a decay rate that is always larger than about 1 month^{-1}. In Figure 1 the dependence of the eigenvalues on $\epsilon_1/(\epsilon_1 + \epsilon_2)$ is shown for fixed $\epsilon^{-1} = \epsilon_1^{-1} + \epsilon_2^{-1}$, with ϵ and the other parameters set to the values obtained in section 3. The fast decay rate is much larger than the slow one. To a good approximation, the slow eigenvalues depend only on ϵ, that is "the relaxation times add up". On the slow manifold, that is the 2-dimensional subspace to which the system trajectories are attracted, h_E is a linear combination of h_W and T_E. The combination depends on the ratio ϵ_1/ϵ_2, in the limit that ϵ_1 is infinite, h_E is proportional to T_E.

[8] T_E and h are natural variables for the slow manifold since the difference $h_E - h_W$ is highly correlated with T_E. Making the approximation $h \approx 0.5(h_W + h_E)$, the slow manifold equations can be written in terms of the natural variables:

$$\begin{aligned} \frac{d}{dt}T_E &= a_{11}T_E + a_{12}h \\ \frac{d}{dt}h &= a_{21}T_E + a_{22}h, \end{aligned} \tag{4}$$

where the coefficients a_{ij} can be obtained from the coefficients in (3) by straightforward algebra.

3. Parameter Fit to Observations

[9] In this section, we estimate with two methods the coefficients in (4) from observations of monthly mean quantities over the period 1980–2002. For T_E we use the observed NCEP Niño3 index [*Reynolds et al.*, 2002], that is the SST anomaly averaged over 5°S–5°N, 150°W–90°W. As a measure for the wind stress τ we use an average of the FSU objective pseudo wind stress [*Smith et al.*, 2004] over 6°S–6°N, 160°E–140°W. For thermocline depth, we use the BMRC data set of the 20° isotherm depth of *Smith* [1995] averaged over 5°S–5°N, h_W the average over 130°E–170°E, h_E the average over 150°W–90°W, and h the average over 130°E–80°W.

[10] In the first method, the equations in (3) are treated separately. The evolution of each variable is estimated by integrating the corresponding equation forward in time from the observed starting value of January 1980, using on the r.h.s. the estimate for the variable and the observed values for the other variables. The parameters are determined from the requirement that they minimize the rms difference between the estimated and observed variables. For the optimal parameters, the correlation between the simulated and the observed variables is around 0.85, except for τ, where it is 0.73. We find r^{-1} = 6.25 month, ϵ_1^{-1} = 2.75 month, ϵ_2^{-1} = 2 month, γ_h = 0.077 K m^{-1}, α = 0.67, b = 14 m K^{-1} ($b\gamma_h$ = 1.1). The short timescales ϵ_1^{-1} and ϵ_2^{-1} are of similar magnitude. So neither wave dynamics nor SST dynamics dominates the time delay between west and east Pacific. Note that for relaxation equations as in (3), the ϵ^{-1} are about twice as large as the lag for which the maximal covariance occurs between the dependent variable and the forcing variable, and also that the values found above depend somewhat on the areas that enter the defi-

nitions of the four basic variables. For the slow manifold, $h_E = 0.67\ h_W + 1.05\ \tau$. This gives for the parameters in (4):

$$\begin{pmatrix} a_{11} & a_{12} \\ a_{21} & a_{22} \end{pmatrix} = \begin{pmatrix} -0.12 & 0.022 \\ -0.94 & 0.004 \end{pmatrix} \tag{5}$$

with T_E in K, h in m, and time in months.

[11] In the second method, the parameters in (4) are obtained from a standard fit that minimizes the rms error of 1-month forecasts of monthly mean values. We used a statistical bootstrap procedure with a 9-month moving block length to estimate 95% CL limits. This method gives:

$$\begin{pmatrix} a_{11} & a_{12} \\ a_{21} & a_{22} \end{pmatrix} = \begin{pmatrix} -0.076 \pm 0.023 & 0.0236 \pm 0.0033 \\ -1.25 \pm 0.13 & -0.008 \pm 0.016 \end{pmatrix}. \tag{6}$$

The agreement between the results obtained by the two methods is reasonable. The consistency between the two methods is evidence for the recharge oscillator model, because in the first method sets of parameters have been fitted with independent criteria instead of assuming the existence of an interannual oscillation. For the original recharge oscillator model the first method gives $a_{11} = -0.17$, $a_{12} = 0.028$, $a_{21} = -1.55$, $a_{22} = 0.038$, which does not agree that well.

[12] We have also tested whether (6) can be used for making ENSO predictions. It was found that the system has considerable skill over persistence, and that using h observations or estimates from wind-driven ocean models increases the forecast skill compared to when only T_E time series information is used (using the method of *Burgers* [1999]), in line with the results obtained by *Xue et al.* [2000] for linear Markov models that include sea-level information.

4. The Simplest Recharge Oscillator

[13] The above result clearly shows that the damping on eastern Pacific temperature T_E is much stronger than the damping on the mean equatorial thermocline depth h. In retrospect, this is not surprising. The damping on T_E is the net result of a number of positive and negative feedbacks, including the Bjerknes feedback. So only by coincidence, this would result in a very small damping or growth rate. A sudden positive perturbation of τ will give rise to Ekman transport that initially deepens the mean equatorial thermocline depth h. On longer timescales, the change in h is mainly governed by the geostrophic response to the wind stress that causes Sverdrup transport to off-equatorial regions, and hardly by the thermocline depth itself. This results in a damping rate that is very close to zero and in a negative a_{21}. For the western equatorial thermocline depth h_W, the damping rate is higher because here also east-west exchanges through wave dynamics play a role.

[14] We scale T_E and h by appropriate factors such that for the scaled variables $a_{21} = -a_{12}$ in (6). This gives:

$$\begin{pmatrix} a_{11} & a_{12} \\ a_{21} & a_{22} \end{pmatrix} = \begin{pmatrix} -0.08 \pm 0.02 & 0.17 \pm 0.02 \\ -0.17 \pm 0.02 & 0.01 \pm 0.02 \end{pmatrix}. \tag{7}$$

Solutions of the weakly damped system (7) follow almost circular trajectories, so we expect that the variances of the scaled T_E and h are of similar magnitude after scaling. In fact, the scaling makes the variances of T_E and h equal within the error estimates. So within the error estimates we can make the approximations $a_{22} = 0$ and $a_{21} = -a_{12}$ when T_E and h are normalized by their variances, and we obtain:

$$\frac{d}{dt}\begin{pmatrix} T_E \\ h \end{pmatrix} = \begin{pmatrix} -2\gamma & \omega_0 \\ -\omega_0 & 0 \end{pmatrix}\begin{pmatrix} T_E \\ h \end{pmatrix} \tag{8}$$

with a period $2\pi\omega^{-1} = 37^{+8}_{-4}$ months and a decay time $\gamma^{-1} = 24^{+22}_{-11}$ months (we have indicated 95% CL limits; note that $\omega^2 = \omega_0^2 - \gamma^2$).

[15] By fitting the linear system (4) to observations, we automatically obtain a weakly damped harmonic oscillator form. However, it should be noted that this result does not necessarily mean that in reality ENSO is a linear damped oscillator excited by stochastic forcing. Weakly damped systems and slightly supercritical systems show very similar behavior in the presence of noise and are hard to distinguish, as for example discussed in *Jin* [1997]. We found above that scaling makes the variances of T_E and h almost equal rather than of similar magnitude as one would expect for a linear system with a damping that is as large as we found. Perhaps this is an indication that the linear fit overestimates the amplitude of the stochastic forcing and in reality non-linearities play a role. Then the near-neutral oscillator could be the result of non-linear equilibration through both deterministic nonlinear dynamics and stochastic fluctuations.

[16] The equations for (T_E, h) of the recharge oscillator (8) are identical to the equations for (p, q) of a classical damped oscillator, with T_E having the role of momentum p and h that of position q. We propose that (8) is the simplest system that contains the essence of ENSO.

5. Seasonal Cycle Effects

[17] Obviously, the system (8) is far from a complete description of ENSO. Only two variables were retained, and even the dynamics of the two variables has been simplified enormously. In particular, in the present analysis non-linear effects are neglected completely, although ENSO fluctuations can be large with respect to the variations in the background state and nonlinearities cause the asymmetry between El Niño and La Niña events [*An and Jin*, 2004]. Also, zonal advection effects on SST are all lumped into the constant ϵ_1 [*Jin and An*, 1999], mirroring the extremely crudely fashion the atmosphere is represented. Finally, our analysis is limited to extracting one oscillating mode.

[18] Perhaps the most important omission is that we have not considered seasonality so far. *Xue et al.* [2000] and *Clarke and van Gorder* [2003] present evidence that including seasonality improves the forecast skill of simple models that use upper ocean heat content. *McPhaden* [2003] discusses the strong seasonality of the autocorrelations and cross correlation of T_E and h. The importance of seasonality is obvious when we make a fit of (4) with parameters that depend on the month of the year. Figure 2 shows the real and imaginary parts γ and ω of the seasonal-dependent eigenvalues. The fluctuations are significant and so large that during some months there are two real roots instead of a pair of complex roots. Boreal spring and fall are relatively

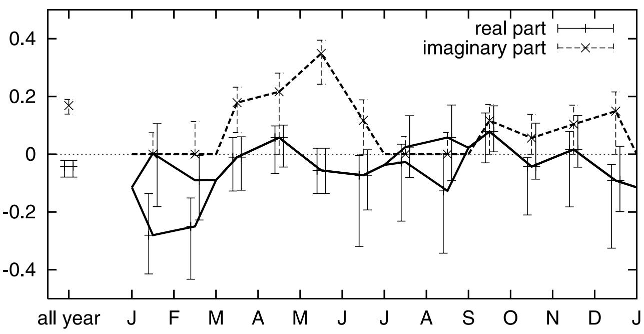

Figure 2. Seasonal cycle in decay constants (solid line: negative for damping, positive for growth) and frequency (dashed line) for the period 1980–2002. Bars denote 95%CL limits determined by a statistical bootstrap procedure.

unstable. In spring the phase progression ω is larger than the annual average, in fall it almost comes to a halt. Interpreting the residues of the fit as noise, the signal-to-noise ratio is largest in fall and smallest in spring because of fluctuations in amplitude (not shown). Both the behavior of the eigenvalues and of the signal-to-noise ratio make El Niño easier to predict through boreal fall than through spring.

6. Conclusion

[19] Observations support that the minimal description of ENSO is a recharge oscillator of equatorial eastern Pacific temperature anomalies T_E and mean equatorial Pacific thermocline depth anomalies h. The ENSO oscillator equation has the very same form as the equation of a classical damped oscillator, with T_E playing the role of momentum and h that of position, and is characterized by two timescales. The first timescale is a characteristic period of 3–4 years, the second timescale an effective decay time of the order of 2 years. In this approximation, basic geostrophy makes that the damping on h is almost zero and its evolution governed by Sverdrup transport due to wind stress anomalies which in turn are directly proportional to T_E. For T_E direct feedbacks such as the Bjerknes feedback of T_E and wind stress anomalies play a role. Both wave dynamics and SST dynamics contribute to the phase difference between T_E and the western equatorial thermocline depth h_W that makes an oscillation possible. During boreal spring, with a large phase progression, and boreal autumn, with nearly stationary phase, the system is more unstable stable than in the remainder of the year.

[20] **Acknowledgment.** Discussions with Henk Dijkstra, Michael Ghil, Michael McPhaden, Huug van den Dool and Yan Xue are gratefully acknowledged.

References

An, S.-I., and F.-F. Jin (2004), Nonlinearity and asymmetry of ENSO, *J. Clim.*, *17*, 2399–2412.
Battisti, D., and A. C. Hirst (1989), Interannual variability in a tropical atmosphere-ocean model: Influence of the basic state, ocean geometry and nonlinearity, *J. Atmos. Sci.*, *46*, 1687–1712.
Burgers, G. (1999), The El Niño Stochastic Oscillator, *Clim. Dyn.*, *15*, 521–531.
Clarke, A., and S. van Gorder (2003), Improving El Niño winds and equatorial Pacific upper ocean heat content, *Geophys. Res. Lett.*, *30*(7), 1399, doi:10.1029/2002GL016673.
Fedorov, A., S. Harper, S. Philander, B. Winter, and A. Wittenberg (2003), How predictable is El Niño?, *Bull. Am. Meterol. Soc.*, *84*, 911–919, doi:10.1175/BAMS-84-7-911.
Jin, F.-F. (1996), Tropical ocean-atmosphere interaction, the Pacific Cold Tongue, and the El Niño/Southern Oscillation, *Science*, *274*, 76–78.
Jin, F.-F. (1997), An equatorial recharge paradigm for ENSO: I. Conceptual model, *J. Atmos. Sci.*, *54*, 811–829.
Jin, F.-F., and S.-I. An (1999), Thermocline and zonal advective feedbacks within the equatorial ocean recharge oscillator model for ENSO, *Geophys. Res. Lett.*, *26*, 2989–2992.
Kessler, W. (2002), Is ENSO a cycle or a series of events?, *Geophys. Res. Lett.*, *29*(23), 2125, doi:10.1029/2002GL015924.
McPhaden, M. (2003), Tropical Pacific Ocean heat content variations and ENSO persistence barriers, *Geophys. Res. Lett.*, *30*(9), 1480, doi:10.1029/2003GL016872.
Mechoso, C., J. Neelin, and J.-Y. Yu (2003), Testing simple models of ENSO, *J. Atmos. Sci.*, *60*, 305–318.
Meinen, C., and M. J. McPhaden (2000), Observations of warm water volume changes in the equatorial Pacific and their relationship to El Niño and La Niña, *J. Clim.*, *13*, 3551–3559.
Neelin, J. D., D. S. Battisti, A. C. Hirst, F.-F. Jin, Y. Wakata, T. Yamagata, and S. E. Zebiak (1998), ENSO theory, *J. Geophys. Res.*, *103*, 14,261–14,290.
Philander, S., and A. Fedorov (2003), Is El Niño sporadic of cyclic?, *Ann. Rev. Fluid Mech.*, *31*, 579–594, doi:10.1146/annurev.earth.31.100901.141255.
Reynolds, R. W., N. Rayner, T. M. Smith, D. Stokes, and W. Wang (2002), An improved in situ and satellite SST analysis for climate, *J. Clim.*, *15*, 1609–1625.
Smith, N. (1995), An improved system for tropical ocean sub-surface temperature analyses, *J. Atmos. Oceanic Technol.*, *12*, 850–870.
Smith, S., J. Servain, D. Legler, J. Stricherz, M. Bourassa, and J. O'Brien (2004), In situ-based pseudo-wind stress products for the tropical oceans, *Bull. Am. Meterol. Soc.*, *85*, 979–994.
Suarez, M., and P. S. Schopf (1988), A delayed action oscillator for ENSO, *J. Atmos. Sci.*, *45*, 3283–3287.
Xue, Y., A. Leetmaa, and M. Ji (2000), ENSO prediction with Markov models: The impact of sea level, *J. Clim.*, *13*, 849–871.
Zelle, H., G. Appeldoorn, G. Burgers, and G. J. van Oldenborgh (2004), The relationship between sea surface temperature and thermocline depth in the eastern equatorial Pacific, *J. Phys. Oceanogr.*, *34*, 643–655.

G. Burgers and G. J. van Oldenborgh, Royal Netherlands Institute of Meteorology (KNMI), P.O. Box 201, NL-3730 AE De Bilt, Netherlands. (burgers@knmi.nl; oldenborgh@knmi.nl)
F.-F. Jin, Department of Meteorology, Florida State University, P.O. Box 4520, Tallahassee, FL 32306-4520, USA. (jff@met.fsu.edu)